Pumped Thermal Energy Storage for Multi-Energy Systems Optimization

Alessandra Ghilardi [a,*], Guido Francesco Frate [a], Antonio Piazzi [b], Mauro Tucci [a], Konstantinos Kyprianidis [c], Lorenzo Ferrari [a]

[a] *Department of Energy, Systems, Territory and Construction Engineering, University of Pisa, Pisa, Italy,*

[b] *i-EM s.r.l., Livorno, Italy,*

[c] *Department of Sustainable Energy Systems, School of Business, Society and Engineering, Malardalen University, Västerås, Sweden,*

* alessandra.ghilardi@phd.unipi.it

Abstract

Grid-scale energy storage systems are essential to support renewables integration and ensure grid flexibility simultaneously. As an alternative to electrochemical batteries, Pumped Thermal Energy Storage is a new storage technology suitable for grid-scale applications. This device stores electric energy as thermal exergy, which can be discharged directly for thermal uses or converted back into power depending on the necessities of the grid. The capability of the proposed energy storage to act as electric and thermal storage fits with the sector coupling necessities of multi-energy systems in which electrical and thermal energy carriers are involved. This paper investigates the effects on optimal grid management of integrating a Brayton Pumped Thermal Energy Storage into a multi-energy system. The case study includes renewable generation from photovoltaic modules and residential and industrial users' electrical and thermal load profiles. The system day-ahead optimization, performed through a Mixed Integer Linear Programming approach, aims to minimize the operational cost computed over a 24-hour horizon. The simulation highlights how the proposed storage technology interacts with the users' requirements during different seasons. The final results highlight that using multi-energy storage (i.e., providing power, heating, and cooling) brings a 5% reduction in operating costs during the year compared to a traditional electric-to-electric storage operation.

1. Introduction

Massive exploitation of Renewable Energy Sources (RES) is essential to fulfil the European Union (EU) climate targets for the 2050 net-zero scenario [1]. As a result of the EU policies aimed to face the climate change of the last two decades, many devices for efficiently exploiting RES are nowadays available, such as photovoltaic (PV) modules and wind turbines. Besides this, properly managing and integrating RES into energy systems is essential for reducing carbon emissions.

Strategies for integrating non-dispatchable RES have traditionally focused on the electric grid side since the introduction of the concept of Smart Grids [2]. Despite that, specific operational and planning strategies should address all other energy sectors and their interactions with the electric grid [3]. In this framework, integrated Multi-Energy Systems (MES) can improve the economic and environmental performance of equivalent independent energy systems [4].

MES can include several energy vectors, such as electric, heating, cooling, fuels and transport, who can interact with each other at a district level. MES usually also involve Energy Storage Systems (ESS), essential devices to enhance the system flexibility and fulfil the users' needs [5]. Among the several ESS solutions, multi-energy storages are particularly suitable for MES [6].

Multi-energy storage can store different energy carriers using the same device, thus potentially achieving better economic and environmental performances than separate devices. Carnot Batteries (CBs) are suitable technologies to accomplish this goal since they store electric energy as thermal exergy, which can be directly used or converted back to electricity [7]. CBs are emerging as an alternative grid-scale storage technology due to their long operational life (20-30 years), low cost per kWh [8] and independence from rare raw materials. Since CBs are gaining interest, many technologies have been proposed in the scientific literature for MES optimization, including Liquid Air Energy Storage (LAES) [9],

Compressed Air Energy Storage (CAES) [10], Rankine-based Pumped Thermal Energy Storage (Ra-PTES) [11], and Brayton-based Pumped Thermal Energy Storage (Br-PTES) [12].

Despite these positive features, the economic advantages of using CBs as a pure electric-to-electric storage capacity are still not clearly assessed [13]. However, using CBs in MES as a multi-energy storage capacity could unlock additional revenue streams, improving the CB economic performance.

Among all the CBs technologies, this paper focuses on Br-PTES, given its high round-trip efficiency (50-70%) [14], compared to LAES and Ra-PTES (40-60%) [15] [16]. Br-PTES uses electric energy to power a Br Heat Pump (HP), which charges a High-Temperature Thermal Energy Storage (HT-TES). The stored thermal exergy can then be used directly for heating purposes or as the hot source to power a Br discharging cycle [17]. An additional thermal reservoir, i.e., a Low-Temperature Thermal Energy Storage (LT-TES), can be used to realize a closed-loop configuration [13]. The latter is particularly interesting for MES applications since coupling the electric, heating and cooling networks is a typical requirement at the city-district level [18].

Various storage configurations utilizing solid and liquid media have been proposed [19]. Liquid media, like molten salts (at temperatures between 500-800 K) and cryogenic hydrocarbons (180-300 K), show good resistance to thermal cycles and effective heat transfer capabilities [20]. On the other hand, solid materials such as magnetite, hematite, concrete blocks and ceramic balls tend to be cheaper and can be used in a broader range of operative temperatures [21] when arranged in arrayed packed beds [22].

Although many Br-PTES configurations have been proposed, their integration in MES is barely investigated. Authors in [23] proposed the modelling and integration of Br-PTES at a domestic scale case study which involves different energy vectors. However, Br-PTES achieve higher efficiency when their size is at the grid-scale level, in which they could become cost-effective and competitive with the Li-ion batteries. For these reasons, this paper proposes a novel investigation at a city-district level. Finally, most papers cited in the literature survey have focused on Br-PTES optimal design. However, since the integration of such storage in real systems is recent, the investigation of the optimized management strategies still lacks proper space in the literature.

The contribution of this paper, then, is to simulate a MES which includes electric, heating and cooling loads, RES generation units (PVs), and a Br-PTES to optimize the energy dispatchment at the city-district level. Given this framework, the results highlight how the storage interacts with each energy vector during the different seasons. As a final result, the paper compares the operating costs achieved by the traditional electric-to-electric operation and the multi-energy operation proposed in this study.

2. Methodology

2.1 System architecture

The case study simulates a likely multi-energy system operating at a city-district level located in Sicily, Italy, encompassing different user types, including 35 residential buildings (100 m^2 each) and non-residential buildings, such as 1 supermarket (5000 m^2 of floor area) and 1 healthcare facility (10000 m^2 of floor area). A schematic representation of the district is given in

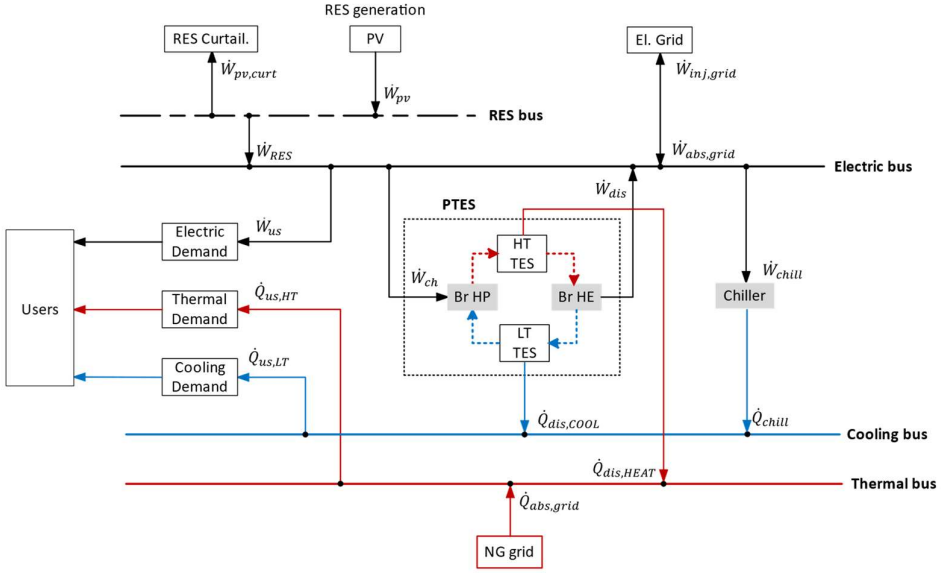

Figure 1. City district model scheme including users' demand, RES production, grid supplies and PTES storage capacity.

Figure 1. Each user is defined by its electric, thermal, and cooling load, with the share of these three vectors varying seasonally. In addition to its reliance on electric and natural gas grids, the system is also equipped with PV modules installed on buildings' rooftops. Finally, the installed storage capacity of the system is provided by a Br-PTES, which can meet the district's electric and heating/cooling necessities.

The electric, heating, and cooling demand profiles are simulated through the software nPro [24]. The software creates the profiles starting from the annual temperature profile (with hourly resolution) of the selected location. By doing so, the electric and thermal profiles are coherent reciprocally and with the outdoor temperature. The latter was provided by the METAR database handled by Iowa Environmental Mesonet [25]. A synthetic overview of the district demands is provided in Table 1.

Concerning the energy prices, ENTSO database [26] and ARERA [27] are used for the cost of absorbed electric energy from the grid, $c_{abs,el}$ measured in €/MWh, and the cost of the absorbed thermal energy from the Natural Gas (NG) grid, $c_{abs,th}$ measured in €/Sm^3.

The PV generation data are simulated starting from the solar radiation data collected from satellite earth observations [28] and processed employing the PVlib library for Python [29] to produce the AC power output. The total installed power of the PV is size 1200 kW, according to the electric and cooling requirements of the district.

Table 1. Electric, heating, and cooling loads of the district

Utility	El. (kW)	Heat (kW)	Cool. (kW)
Residential	112	544	313
Hospital	230	1044	950
Supermarket	69	629	418

2.2 Br-PTES storage

The Br-PTES charging and discharging phases are realized through inverse and direct Brayton-Joule cycles, Brayton Heat Pump (Br-HP) and Brayton Heat Engine (Br-HE), respectively, as represented in Figure 2. Argon is used as the working fluid since it is one of the most common fluids investigated in the literature [30], thanks to its capability of reaching higher temperatures with the same pressure level as other competitive fluids (like helium, nitrogen and air), thus increasing the round-trip efficiency. The HP and the HE operate between a maximum and minimum temperature equal to 500 °C and -80 °C, respectively, thanks to the HT TES and LT TES that act as thermal reservoirs. The storage technology is modelled by defining specific charging and discharging parameters for the HT and LT TES, α_{dis} and α_{ch}, which links the charging and discharging heat flow rates of the TES to the electric charging and discharging net power of charging and discharging phases. Equation (1) and Equation (2) show the definition of these coefficients, where $\bar{\dot{W}}_{ch}$, $\bar{\dot{W}}_{dis}$ are the nominal net power, given by the difference between the compressor charging input power and the turbine discharging output power or vice versa. $\bar{\dot{Q}}_{ch,HT}$ and $\bar{\dot{Q}}_{dis,HT}$ are instead the associated nominal thermal power for charging or discharging the HT TES.

$$\alpha_{ch,HT} = \frac{\bar{\dot{Q}}_{ch,HT}}{\bar{\dot{W}}_{ch}};\ \alpha_{dis,HT} = \frac{\bar{\dot{Q}}_{dis,HT}}{\bar{\dot{W}}_{dis}} \quad (1)$$

$$\alpha_{ch,LT} = \frac{(1-\bar{\dot{Q}}_{ch,HT})}{\bar{\dot{W}}_{ch}};\ \alpha_{dis,LT} = \frac{(1-\bar{\dot{Q}}_{dis,HT})}{\bar{\dot{W}}_{dis}} \quad (2)$$

These coefficients are determined by modelling the charging and discharging thermodynamic cycles by assuming the maximum and minimum cycle temperatures (T_{max} and T_{min}), the iso-entropic efficiency of the compressor, $\eta_{is,c}$, and the turbine $\eta_{is,t}$, and the ratio between the maximum and minimum pressure of the cycles, β, as summarised in Table 2.

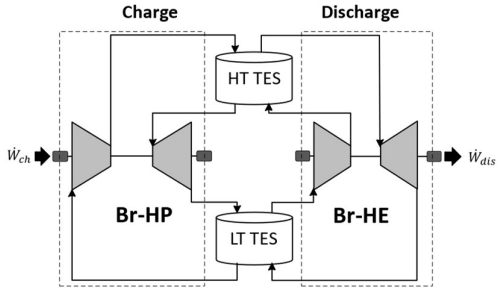

Figure 2. Br-PTES configuration with charge and discharge phases realized by the Br HP and the Br HE, respectively.

The storage model can simulate different operative conditions. Once the storage is charged through electric input by powering the compressor of the HP, the discharge phase can indeed release other vectors, as follows:

- **Electric-to-electric.** The HT and LT tanks act as hot and cold reservoirs to operate a direct Brayton-Joule thermodynamic cycle, which produces electric energy.
- **Electric-to-heating**. The exergy stored in the HT-TES is directly used to fulfil the heating requirements of the district.
- **Electric-to-cooling**. The exergy stored in the LT-TES is directly used to fulfil the cooling requirements of the district.

Table 2. Charging and discharging cycle parameters for the determination of α_{dis} and α_{ch} with Argon as working fluid. Values based on [30].

Parameter	Value
T_{max}	500 °C
T_{min}	-80 °C
β(ch/dis)	4.56/6.54 (-)

$\eta_{is,c}$	0.87 (-)
$\eta_{is,t}$	0.92 (-)

2.3 Sizing of the components

Given the case study's electrical demand and RES production, the storage nominal power ratings, $\bar{\dot{W}}_{ch}$ and $\bar{\dot{W}}_{dis}$, are calculated by a preliminary analysis based on the duration curves of the absolute difference between the electric demand and the RES generation. Particularly, $\bar{\dot{W}}_{ch}$ and $\bar{\dot{W}}_{dis}$ are chosen to match the charging/discharging power required 80% of the time. The charging and discharging durations, τ_{ch}, τ_{dis} are set equal to 6 hours and 3 hours, respectively, which are typical values for RES integration purposes. From these, the nominal HT and LT TES capacities are calculated as in Equation (3):

$$\bar{C}_{HT} = \bar{C}_{LT} = \bar{\dot{W}}_{dis} \cdot \left(\frac{1}{\alpha_{dis}} - 1\right) \cdot \tau_{dis} \quad (3)$$

Concerning the other components of the district, the nominal power absorbed from the electric and NG grids and by the chiller are equal to the maximum of the electric, heating, and cooling demand, respectively, as follows: $\bar{\dot{W}}_{abs,grid} = \max(\dot{W}_{dem})$, $\bar{\dot{Q}}_{abs,grid} = \max(\dot{Q}_{us,HT})$ and $\bar{\dot{Q}}_{chi} = \max(\dot{Q}_{us,LT})$.

Table 3. Storage sizing parameters

Parameter	Value
$\bar{C}_{HT}$	1000 kWh
$\bar{C}_{LT}$	1000 kWh
α_{dis}(HT/LT)	2.7/1.7 (-)
α_{ch}(HT/LT)	1.8/0.8 (-)
$\bar{\dot{W}}_{dis}$	200 kW
$\bar{\dot{W}}_{ch}$	200 kW
τ_{ch}	6 h
τ_{dis}	3 h

2.4 MILP problem formulation

The optimization is realized using a Mixed Integer Linear Programming (MILP) approach, representing state-of-the-art MES optimization techniques. MILP guarantees to find the global optimum in the feasible region Ω, assuming the objective function f_{obj} and the constraints to be linear, and the optimization variables $\boldsymbol{x}$ to be continuous or binary ([0,1] domain). The optimization problem aims to minimize the Operational Cost (OC) and is solved with an hourly timestep t among a 24-hour optimization horizon ($\bar{T}$). The optimization problem is formulated as in Equation. (4), where f_{obj} is given by the sum of the economic losses $\sum_{t=1}^{\bar{T}}\left[\dot{W}_{abs,grid}(t) \cdot c_{abs,el}(t) + \dot{Q}_{abs,grid}(t) \cdot c_{abs,th}(t)\right] \cdot \Delta t$ minus the economic gain $\sum_{t=1}^{\bar{T}}\left[\dot{W}_{inj,grid}(t) \cdot c_{inj,el}(t)\right] \cdot \Delta t$, where $\dot{W}_{abs,grid}$ and $\dot{W}_{inj,grid}$ are the absorbed and injected electric power from the grid, and $\dot{Q}_{abs,grid}$ is the heat flow rate absorbed by the NG grid.

$$\min_{\boldsymbol{x} \in \Omega \in \mathbb{R}^n} \sum\nolimits_{year} (f_{obj}) \quad (4)$$

The optimization algorithm finds the optimal values of the optimization variables $\boldsymbol{x}$, among which the most important ones are:

- $\dot{W}_{ch}$ and $\dot{W}_{dis}$: the charging and discharging power rate for the Br-PTES
- $\dot{W}_{abs,grid}$ and $\dot{Q}_{abs,grid}$: the electrical and thermal heat flow rate provided by the electric and NG grids, respectively.
- The RES curtailment and the PV power input to the electric bus: $\dot{W}_{PV,curt}$ and $\dot{W}_{RES}$, respectively
- Integer variable controlling the on-off status of the storage k_{onoff} (1 is on, 0 is off)
- Integer variable controlling the charging or discharging mode of the PTES, k_{ch} and k_{dis}
- Integer variables controlling the electrical or thermal discharging mode of the storage, k_{el} and k_{th}

Regarding the constraints, the energy balances on the electric, thermal, cooling and RES busses are necessary to guarantee the users' demand fulfilment. Beyond those, some specific constraints characterize the PTES operation. The following list summarizes the most important ones:

- $k_{ch} + k_{dis} \leq k_{onoff,ptes}$. The charging and discharging phases are mutually exclusive (i.e., when the charge is on, the discharge is off, and vice versa)
- $k_{th} + k_{el} \leq k_{dis}$. The electrical and thermal discharges are mutually exclusive (i.e., when the thermal/cooling discharge is on, the electrical discharge is off)
- The State of Charge SOC_k of the k-component (i.e., HT and LT TES) is cyclic over the optimization horizon $\bar{T}$ (Equation 6) and is limited within a $SOC_{k,max}$ and $SOC_{k,min}$ (Equation 5).

$$SOC_{k,min} \leq SOC_k(t) \leq SOC_{k,max} \quad (5)$$

$$SOC_k(t = 0) = SOC_k(\bar{T}) \quad (6)$$

- The charging heat flow rate $\dot{Q}_{ch,k}$ that goes in the HT and LT TES during the charging phase are related to the charging electric heat flow rate, $\dot{W}_{ch}$, by specific coefficients $\alpha_{ch,k}$, which are constant with the HP load, as expressed in Equation (1). The same constraint is valid for the discharging heat flow rates as expressed in Equation (2).

- The SOC of the k-component changes according to the incoming and outcoming heat flow rates, as in Equation (7) and (8), where $\bar{C}_k$ is the TES capacity and $\dot{Q}_{dis,th}$ is the thermal discharge equal to $-\dot{Q}_{dis,HEAT}$ and $+\dot{Q}_{dis,COOL}(t)$ for the HT and LT TES, respectively.

$$SOC_k = SOC_k(t-1) + \Delta SOC_k(t) \quad (7)$$

$$\Delta SOC_k(t) = \frac{\dot{Q}_{ch,k}(t) - \dot{Q}_{dis,k}(t) \pm \dot{Q}_{dis,th}(t)}{\bar{C}_k} \cdot \Delta t \quad (8)$$

- The heat flow rate $\dot{Q}_{chill}$ given by the chiller is related to the electric power absorbed by the electric bus $\dot{W}_{chill}$ by a Energy Efficiency Ratio (EER), which is supposed to be constant with the load. The EER value is set to 3, which is a typical efficiency for chillers for building applications.

3. Results and discussion

3.1 Simulated operation

The optimization process yields the optimal dispatching of the three energy vectors (i.e., electric, thermal, and cooling) the storage delivers. Figure 3 and Figure 4 show a summer and winter representative period, respectively, in which the storage operation faces some typical seasonal patterns of the district energy production and demand. The interaction with the PV production is visible, especially during the summer when the surplus caused by the RES integration is generally used to charge the storage, which is later discharged according to the necessities of the district. For the summer scenario, the electrical discharges usually happen during the first hours of the day, when the air conditioning units of the non-commercial building (supermarket, hospital) are switched on, causing a consumption peak when the PV production is not yet significant. Electrical discharges also happen in the late afternoon when RES production decreases. In that period of the day, the cooling discharges also occur to meet the cooling demand, which is still high (considering the location of the case study). It is worth noting that in the summer period, the storage covers part of the heating load during the central part of the day (required especially in the domestic building for domestic hot water). In this case, indeed, the cooling load is fulfilled by the electric bus, which benefits from the PV production, and the storage then fulfils the heating load to lower its State Of Charge (SOC) and be able to be charged by the surplus in the following timestep. Despite the storage covering part of the cooling load as described, its contribution to the district cooling requirements is limited to a couple of hours in the daytime. This behaviour is because the separate chiller installed in the district works with a higher energy efficiency ratio than the one of the PTES (3 versus 1.7). For this reason, the optimizer chooses to directly exploit the electric grid during the daytime when there is a surplus produced by the RES because it is more convenient and uses the cold stored in the LT TES in the evening hours when the RES production is low.

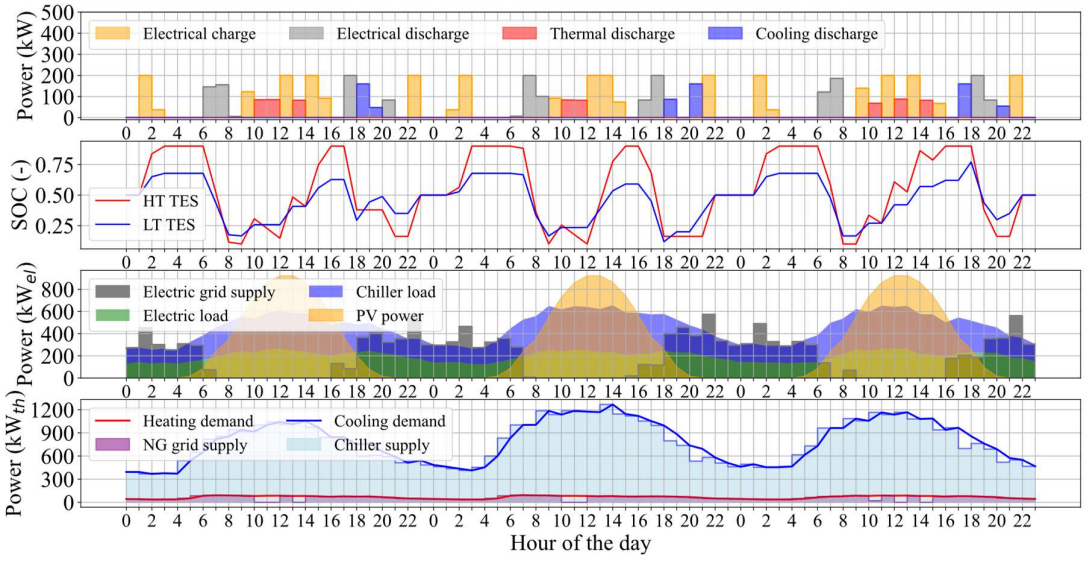

Figure 3. Summer scenario. First image represents the charge/discharge power rates of the storage; second image the SOC of HT and LT storages, third image the electric load fulfillment; forth image the thermal load fulfillment.

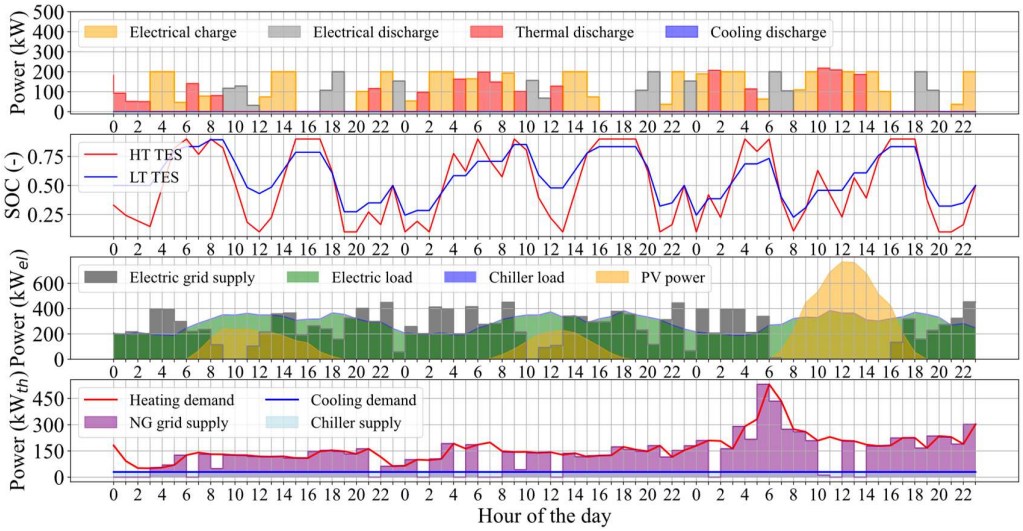

Figure 4. Winter scenario. First image represents the charge/discharge power rates of the storage; second image the SOC of HT and LT storages, third image the electric load fulfillment; forth image the thermal load fulfillment.

A different behavior, instead, happens in the winter scenario. In this case, the PTES significantly contributes to the fulfillment of the heating load, exploiting the HT TES for 5-6 hours per day in the thermal discharge mode. The HT TES, indeed, charges and discharges heat with a higher efficiency compared to LT TES (see values for α_{dis} and α_{ch} in Table 2). Since the LT TES acts as the cold reservoir, indeed, has a limited operation compared to the HT TES, which is the hot reservoir for the involved thermodynamic cycle. This is the reason why the LT TES SOC (visible both in Figure 3 and Figure 4) is not able to follow the HT TES SOC. In other terms, for an equal electrical charge/discharge, the SOC slope of the LT TES is always smaller than the SOC slope of the HT TES. This results in a worse exploitation of the storage capacity, i.e., the SOC of the LT TES varies in a more limited range compared to the HT TES. As a final result, the PTES contribution for the heating is more significant than the one for the cooling.

Besides the RES production, the thermal and electricity prices also affect the storage operation. Both summer and winter scenarios show that sometimes the storage is charged directly from the electric grid during the night-time, buying surplus electricity compared to the electric load. This is due to the lower energy price, which characterizes the night hours. Focusing on the winter scenario, the storage is charged during the night and releases thermal discharge during the first hours of the morning, where the space heating units work with maximum power to heat residential and non-residential buildings. Finally, the electrical discharges happen mostly during the late afternoon, when an electric consumption peak occurs.

3.2 Impact of multi-energy storage operation

The previous section provided a qualitative analysis of the PTES contribution to the analyzed MES, showing a three-day sample period. However, the final purpose of the simulation is to estimate the benefits of using multi-energy storage for a MES application. For this reason, this section provides a quantitative yearly comparison between the PTES operating as a traditional Electric-to-Electric (E-E) storage and the proposed concept of Electric-to-Electric/Heating (E-E/H) or Electric-to-Electric/Heating/cooling (E-E/H/C) storage. Figure 5 compares these three cooperative conditions in terms of OC. The results are normalized with the operating costs in case of no storage capacity installed in the system (OC_0). As the plot clearly shows, the operational costs are reduced when the PTES interacts with the district to provide electricity, heating, and cooling. The only E-E operative condition provides significant cost reduction compared to the no storage case by lowering the OC by 5%. Introducing the E-E/H and E-E/H/C modalities provides an additional

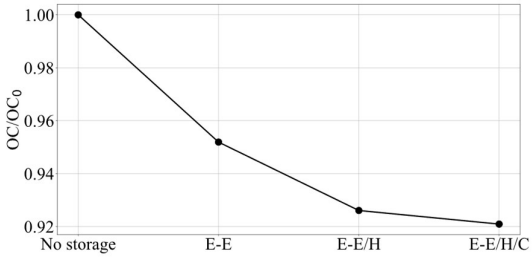

Figure 5. Yearly operating cost for different Operative Costs (OC) of the PTES. Electric-to-Electric (E-E), Electric-to-Electric/Heating (E-E/H) and Electric-to-Electric/Heating/Cooling (E-E/H/C). The subscript 0 refers to the case of no storage capacity.

reduction in the OC, equal to 2% and 1%, respectively. It is worth noting that the E-E/H/C mode brings to a limited improvement of the overall OC, because the PTES works as cold storage for a limited number of hours during the year. This phenomenon occurs due to the limited performance of the LT TES, as discussed in the previous section. Anyway, as a final result, the PTES working as a multi-energy storage is able to reduce the OC of 8% overall.

4. Conclusions

The present work aims to simulate the integration of Brayton-based PTES storage in a multi-energy system at a city-district size, which involves electric, heating, and cooling demand. The system operation was optimized through a Mixed Integer Linear Programming approach to minimize the operating costs. The qualitative results of the simulation showed that the PTES properly interacts with the community by delivering the optimal share of electric, heating, and cooling discharges to fulfil the demand. Beyond that, the quantitative analysis highlighted that using the PTES as a multi-storage capacity significantly reduces the operating costs compared to only electric-to-electric usage, typically proposed for this technology [13]. Comparing these results with the literature, it is found that similar performances (overall operative cost reduction around 10%) were already achieved in [11], by adopting a MILP formulation as well and using a Ra-PTES storage device. However, the cited paper highlights that including the capital costs makes the PTES technology less cost-effective than traditional Li-ion batteries. These findings, then, encourage further analysis to compare the Br-PTES with the other grid-scale technologies, and better define its potential for MES applications. Basing on the benefits showed in the results section, indeed, the proposed storage technology gives support to the idea of enhancing energy communities within multi-energy vector concept, which has been already supported by the new Eu policies.

It is worth to note that the discussed results are related to the single selected case study (i.e., fixed RES, load profiles and storage capacity). Further sensitivity analysis on the storage size, RES penetration and RES profiles (e.g., wind generation beyond solar radiation) could help better define the most suitable application for Br-PTES at a city district level. Finally, from a modelling point of view, this study only considers a first law approach (i.e., only energy exchanges are included in the model). It would then be interesting, as a further step, to evaluate the actual performances of the system when heat is exchanged under temperature differences and assess the potential of Br-PTES with different temperature levels on the demand side.

Acknowledgement

This research has received financial contribution from the Italian Operative National Plan (Piano Operativo Nazionale, PON) in the framework of the project Ricerca e Innovazione 2014−2020 (PON R&I) – Azione IV.6 “Contratti di ricerca su tematiche dell'innovazione e green” (DM MUR 1062/2022).

Project funded under the National Recovery and Resilience Plan (NPRR), Mission 4 Component 2 Investment 1.3 – Call for tender No. 1561 of 11.10.2022 of Ministero dell’Università e della Ricerca (MUR); funded by European Union – NextGenerationEU.

Acronyms and abbreviations

Br	Brayton-Joule
CAES	Compressed Air Energy Storage
CB	Carnot Battery
COOL	Cooling
E-E	Electric to Electric
E-E/H	Electric to Electric/Heating
E-E/H/C	Electric to Electric/Heating/Cooling
EER	Energy Efficiency Ratio
ESS	Energy Storage System
EU	European Union
HE	Heat Engine
HEAT	Heating
HP	Heat Pump
HT	High Temperature
LAES	Liquid Air Energy Storage
LT	Low Temperature
MES	Multi Energy System
MILP	Mixed Integer Linear Programming
NG	Natural Gas
OC	Operating Cost
ORC	Organic Rankine Cycle
PTES	Pumped Thermal Energy Storage
PV	Photovoltaic
Ra	Rankine
RES	Renewable Energy Sources
SOC	State of Charge
TES	Thermal Energy Storage

Symbols

α	Electric to heating/cooling power
β	Compression ratio
c	Cost
$\bar{C}$	Nominal storage capacity
Δ	Difference
f	Function
η	Efficiency
k	Binary optimization variable
Ω	Feasible region
$\dot{Q}$	Thermal power
$\bar{\dot{Q}}$	Nominal thermal power
T	Temperature
$\overline{T}$	Optimization horizon

τ	Duration
t	Time
$\dot{W}$	Electric power
$\bar{\dot{W}}$	Nominal electric power
x	Continous optimization variables

Subscripts

abs	Absorbed
c	Compressor
ch	Charge
chill	Chiller
curt	Curtailment
dem	Demand
dis	Discharge
el	Electric
inj	Injected
is	Iso-entropic
min	Minimum
max	Maximum
obj	Objective
onoff	On-off status
t	Turbine
th	Thermal
us	Users
0	Base-line scenario

References

[1] 2050 long-term strategy n.d. https://climate.ec.europa.eu/eu-action/climate-strategies-targets/2050-long-term-strategy_en (accessed June 5, 2023).

[2] Tuballa ML, Abundo ML. A review of the development of Smart Grid technologies. Renew Sustain Energy Rev 2016;59:710–25. https://doi.org/10.1016/j.rser.2016.01.011.

[3] Mancarella P. Smart Multi-Energy Grids : Concepts , Benefits and Challenges 2012:9–10.

[4] Mancarella P. MES (multi-energy systems): An overview of concepts and evaluation models. Energy 2014;65:1–17. https://doi.org/10.1016/j.energy.2013.10.041.

[5] Victoria M, Zhu K, Brown T, Andresen GB, Greiner M. The role of storage technologies throughout the decarbonization of the sector-coupled European energy system. Energy Convers Manag 2019;201:111977. https://doi.org/10.1016/j.enconman.2019.111977.

[6] Nozari MH, Yaghoubi M, Jafarpur K, Mansoori GA. Development of dynamic energy storage hub concept: A comprehensive literature review of multi storage systems. J Energy Storage 2022;48:103972. https://doi.org/10.1016/j.est.2022.103972.

[7] Dumont O, Frate GF, Pillai A, Lecompte S, De paepe M, Lemort V. Carnot battery technology: A state-of-the-art review. J Energy Storage 2020;32. https://doi.org/10.1016/j.est.2020.101756.

[8] Frate GF, Ferrari L, Desideri U. Energy storage for grid-scale applications: Technology review and economic feasibility analysis. Renew Energy 2021;163:1754–72. https://doi.org/10.1016/j.renene.2020.10.070.

[9] Vecchi A, Li Y, Mancarella P, Sciacovelli A. Multi-energy liquid air energy storage: A novel solution for flexible operation of districts with thermal networks. Energy Convers Manag 2021;238:114161. https://doi.org/10.1016/j.enconman.2021.114161.

[10] Cheng Y, Liu M, Chen H, Yang Z. Optimization of multi-carrier energy system based on new operation mechanism modelling of power-to-gas integrated with CO2-based electrothermal energy storage. Energy 2021;216:119269. https://doi.org/10.1016/j.energy.2020.119269.

[11] Frate GF, Ferrari L, Sdringola P, Desideri U, Sciacovelli A. Thermally integrated pumped thermal energy storage for multi-energy districts: Integrated modelling, assessment and comparison with batteries. J Energy Storage 2023;61:106734. https://doi.org/10.1016/j.est.2023.106734.

[12] Zhang H, Wang L, Lin X, Chen H. Combined cooling, heating, and power generation performance of pumped thermal electricity storage system based on Brayton cycle. Appl Energy 2020;278:115607. https://doi.org/10.1016/j.apenergy.2020.115607.

[13] Mctigue JD, Farres-antunez P, J KS, Markides CN, White AJ. Techno-economic analysis of recuperated Joule-Brayton pumped thermal energy storage. Energy Convers Manag 2022;252:115016. https://doi.org/10.1016/j.enconman.2021.115016.

[14] Steinmann WD, Bauer D, Jockenhöfer H, Johnson M. Pumped thermal energy storage (PTES) as smart sector-coupling technology for heat and electricity. Energy 2019;183:185–90. https://doi.org/10.1016/j.energy.2019.06.058.

[15] Aneke M, Wang M. Energy storage technologies and real life applications – A state of the art review. Appl Energy 2016;179:350–77. https://doi.org/10.1016/j.apenergy.2016.06.097.

[16] Dumont O, Lemort V. Mapping of performance of pumped thermal energy storage (Carnot battery) using waste heat recovery. Energy 2020;211:118963. https://doi.org/10.1016/j.energy.2020.118963.

[17] Olympios A V, McTigue JD, Farres-Antunez P, Tafone A, Romagnoli A, Li Y, et al. Progress and prospects of thermo-mechanical energy storage—a critical review. Prog Energy 2021;3:022001. https://doi.org/10.1088/2516-1083/abdbba.

[18] Ascione F, Canelli M, Francesca R, Masi D, Sasso M, Peter G. Combined cooling , heating and power for small urban districts : An Italian case-study. Appl Therm Eng 2020;71:705–13. https://doi.org/10.1016/j.applthermaleng.2013.10.058.

[19] White A, Parks G, Markides CN. Thermodynamic analysis of pumped thermal electricity storage. Appl Therm Eng 2013;53:291–8. https://doi.org/10.1016/j.applthermaleng.2012.03.030.

[20] Laughlin RB. Pumped thermal grid storage with heat exchange. J Renew Sustain Energy 2017;9. https://doi.org/10.1063/1.4994054.

[21] Zhao Y, Song J, Liu M, Zhao Y, Olympios A V., Sapin P, et al. Thermo-economic assessments of pumped-thermal electricity storage systems employing sensible heat storage materials. Renew Energy 2022;186:431–56. https://doi.org/10.1016/j.renene.2022.01.017.

[22] McTigue JD, Markides CN, White AJ. Performance response of packed-bed thermal storage to cycle duration perturbations. J Energy Storage 2018;19:379–92. https://doi.org/10.1016/j.est.2018.08.016.

[23] Zhang H, Wang L, Lin X, Chen H. Combined cooling, heating, and power generation performance of pumped thermal electricity storage system based on Brayton cycle. Appl Energy 2020;278:115607. https://doi.org/10.1016/j.apenergy.2020.115607.

[24] Wirtz M. nPro: A web-based planning tool for designing district energy systems and thermal networks. Energy 2023;268:126575. https://doi.org/10.1016/j.energy.2022.126575.

[25] Iowa Environmental Mesonet n.d. https://mesonet.agron.iastate.edu/ (accessed June 2, 2023).

[26] ENTSO-E Transparency Platform n.d. https://transparency.entsoe.eu/ (accessed June 2, 2023).

[27] ARERA - Prezzi e tariffe n.d. https://www.arera.it/it/prezzi.htm# (accessed June 2, 2023).

[28] Meteosat series | EUMETSAT n.d. https://www.eumetsat.int/our-satellites/meteosat-series (accessed June 2, 2023).

[29] F. Holmgren W, W. Hansen C, A. Mikofski M. Pvlib Python: a Python Package for Modeling Solar Energy Systems. J Open Source Softw 2018;3:884. https://doi.org/10.21105/joss.00884.

[30] Frate GF, Ferrari L, Desideri U. Techno-Economic Comparison of Brayton Pumped Thermal Electricity Storage (PTES) Systems Based on Solid and Liquid Sensible Heat Storage. Energies 2022;15. https://doi.org/10.3390/en15249595.